Available online at www.sciencedirect.com
ScienceDirect
Comput. Methods Appl. Mech. Engrg. 310 (2016) 460–474
Computer methods in applied mechanics and engineering
www.elsevier.com/locate/cma

A weak penalty formulation remedying traction oscillations in interface elements

Erik Svenning

Division of Material and Computational Mechanics, Department of Applied Mechanics, Chalmers University of Technology, Gothenburg, Sweden

Received 6 April 2016; received in revised form 4 July 2016; accepted 11 July 2016
Available online 28 July 2016

Abstract

A frequently used approach to modeling of fracture along predefined paths (e.g. grain boundaries in metals) is to use intrinsic interface elements. Despite their popularity, it is well known that the use of such elements in combination with a stiff cohesive zone model may result in traction oscillations. A common strategy to alleviate this problem is to employ reduced Lobatto integration along the cohesive surface. Even though such reduced integration has been demonstrated to work well for some cases, the present work shows that there are situations where the use of this integration method results in severe traction oscillations. More precisely, it is shown that intrinsic interface elements (with full or reduced integration) share stability properties with an equivalent mixed formulation, and hence oscillations result from the violation of the inf–sup (LBB) condition for the mixed formulation. As a remedy for these oscillations, the interface elements are modified using a weak penalty formulation, based on a traction approximation fulfilling the inf–sup condition. Using this method, oscillation free results can be obtained without modifying the cohesive zone law or introducing additional unknowns. These oscillation free results are demonstrated by several numerical examples, including straight, curved and intersecting cracks.

Keywords: Interface elements; Traction oscillations; Inf–sup; LBB; Weak penalty

1. Introduction

Intrinsic interface elements allow the modeling of cracks that follow a pre-defined path. Due to its engineering relevance, this approach has attracted considerable research interest for many years, and it is well known that spurious traction oscillations may appear along the interface [1–3]. A popular solution, which seems to have emerged as the standard strategy to overcome this problem [1,2,4,5], is to employ reduced Lobatto integration. Even though the stability of this integration scheme is discussed in several publications (see e.g. [1,6]), the analysis tends to focus on straight cracks without branches or intersections. Hence, the occurrence of traction oscillations for curved and intersecting cracks deserves further investigation.

Several studies have shown that the spurious oscillations occur when the cohesive zone is very stiff [1,3,5], which is often the case in practice. This high stiffness keeps the opening of the element to a minimum in the elastic regime,

E-mail address: erik.svenning@chalmers.se.

http://dx.doi.org/10.1016/j.cma.2016.07.031
0045-7825/

which means that intrinsic interface elements represent a penalty formulation. To overcome the spurious oscillations occurring when using the penalty formulation, an alternative is to employ a mixed formulation, where the cohesive traction along the interface is introduced as an additional unknown field, see e.g. [7,8] in the context of interface elements or [9,10] in combination with the eXtended Finite Element Method (XFEM). Using a mixed formulation allows for modeling of rigid interfaces, however at the cost of additional computational effort and a more complicated formulation of the cohesive zone model. In particular, the cohesive zone model needs to be formulated on compliance format, which makes models exhibiting softening problematic to use in this setting. Nevertheless, a mixed formulation allows for choosing traction approximations that are stable in terms of the inf–sup condition, leading to oscillation-free results.

The advantages of the penalty formulation and mixed formulations can be combined by using a weak penalty (sometimes called interior penalty) formulation, see e.g. [11] for a general discussion or [12] in the context of incompressible elasticity. More precisely, the weak penalty formulation retains the displacement based format, and would thereby allow the modeling of softening in the cohesive zone. More importantly, oscillation-free results can be obtained by fulfilling the inf–sup condition. Specifically, by applying this formulation to interface elements, the constraint corresponding to the interface traction (i.e. the displacement jump in the element, penalized by the high initial stiffness) would be applied in a weak sense, e.g. on average over one or several elements. Hence, the constraint could be weakened in order to fulfill the inf–sup condition. This is in contrast to using a conventional penalty formulation, in which the constraint is applied pointwise in each quadrature point. Hence, applying a weak penalty formulation to intrinsic interface elements would give a possibility to overcome spurious traction oscillations.

Since previous research has focused on traction oscillations for a single smooth crack, the present work investigates such oscillations also for intersecting cracks, and proposes a way to reduce these oscillations using a weak penalty formulation. In particular, it is shown that the conventional intrinsic interface elements with penalty formulation are obtained as a special case of a weak penalty formulation, and that spurious traction oscillations are related to violation of the inf–sup condition. Based on these results, stable choices for the traction approximation are discussed and a weak penalty formulation that leads to oscillation free traction profiles is proposed. In addition to being stable, the proposed formulation does not require modifications to the cohesive zone model and does not introduce additional global unknowns.

The remainder of the paper is organized as follows. The displacement based format pertinent to conventional interface elements is stated in Section 2.1, followed by Section 2.2 where the conventional mixed format is presented and a nonstandard mixed format is proposed. The weak penalty format is derived in Section 2.3. Section 2.4 contains a discussion on situations where the conventional penalty formulation leads to spurious traction oscillations and how to resolve these oscillations by choosing a stable traction approximation and applying it in a weak penalty setting. Numerical examples supporting the theoretical results are given in Section 3 and the discussion in Section 4 concludes the paper.

2. Theory

2.1. Displacement based format

To establish the displacement based weak format, leading to standard interface elements, we consider a domain Ω with boundary $\partial\Omega = \Gamma_{ext} \cup \Gamma_{int}^{+} \cup \Gamma_{int}^{-}$, where $\Gamma_{int} \overset{\text{def}}{=} \Gamma_{int}^{+} \cup \Gamma_{int}^{-}$ represents internal boundaries and Γ_{ext} is the external boundary. Hence, the internal boundaries Γ_{int}, representing cohesive cracks in the material, consist of a positive side Γ_{int}^{+} and a negative side Γ_{int}^{-}, as shown in Fig. 1. The crack normal $\boldsymbol{n}_{int}$ is taken as the outward unit normal on Γ_{int}^{-}, that is $\boldsymbol{n}_{int} \overset{\text{def}}{=} \boldsymbol{n}_{int}^{-}$. The cracks may branch and intersect, hence $\boldsymbol{n}_{int}$ is not necessarily continuous along the crack, not even prior to introducing a Finite Element discretization. Considering small strains and quasistatic loading, the strong form of the equilibrium equations is given by

$$\begin{aligned} -\boldsymbol{\sigma} \cdot \nabla &= \mathbf{0} \text{ in } \Omega, \\ \boldsymbol{t}^{+} + \boldsymbol{t}^{-} &= \mathbf{0} \text{ on } \Gamma_{int}, \\ \boldsymbol{t} \overset{\text{def}}{=} \boldsymbol{\sigma} \cdot \boldsymbol{n} &= \hat{\boldsymbol{t}} \text{ on } \Gamma_{ext,N}, \\ \boldsymbol{u} &= \hat{\boldsymbol{u}} \text{ on } \Gamma_{ext,D}, \end{aligned} \tag{1}$$

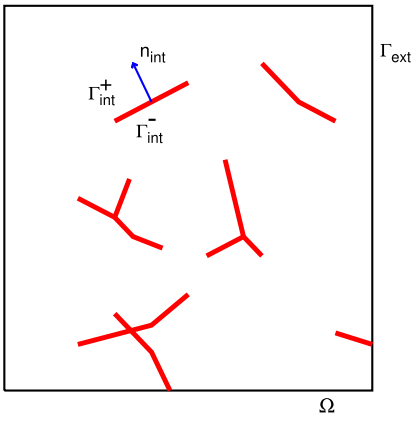

Fig. 1. Domain Ω with boundary $\partial\Omega = \Gamma_{ext} \cup \Gamma^{+}_{int} \cup \Gamma^{-}_{int}$, where Γ^{+}_{int} and Γ^{-}_{int} represent internal boundaries.

where $\boldsymbol{\sigma} = \boldsymbol{\sigma}\left([\boldsymbol{u} \otimes \boldsymbol{\nabla}]^{sym}\right)$ is the Cauchy stress, $\boldsymbol{\nabla}$ is the gradient operator, $\boldsymbol{n}$ is a unit normal vector, $\hat{\boldsymbol{t}}$ is a prescribed traction and $\hat{\boldsymbol{u}}$ is a prescribed displacement. The traction on the internal boundaries Γ_{int} is described by a cohesive zone law specifying $\boldsymbol{t} \overset{\text{def}}{=} \boldsymbol{t}^{+} = -\boldsymbol{t}^{-}$ in terms of the jump $[\![\boldsymbol{u}]\!] \overset{\text{def}}{=} \boldsymbol{u}^{+} - \boldsymbol{u}^{-}$ over the crack faces.

The one field weak solution corresponding to Eq. (1) is obtained by finding $\boldsymbol{u} \in \mathbb{U}$ such that

$$a\left(\boldsymbol{u}, \delta\boldsymbol{u}\right) - b\left(\boldsymbol{t}\left([\![\boldsymbol{u}]\!]\right), \delta\boldsymbol{u}\right) = l\left(\delta\boldsymbol{u}\right) \;\; \forall \delta\boldsymbol{u} \in \mathbb{U}^{0},$$

$$\mathbb{U} = \left\{ \boldsymbol{v} : \boldsymbol{v} \in \left[\mathbb{H}^{1}\left(\Omega\right)\right]^{d}, \;\; \boldsymbol{v} = \hat{\boldsymbol{u}} \text{ on } \Gamma_{ext,D} \right\}, \tag{2}$$

$$\mathbb{U}^{0} = \left\{ \boldsymbol{v} : \boldsymbol{v} \in \left[\mathbb{H}^{1}\left(\Omega\right)\right]^{d}, \;\; \boldsymbol{v} = \boldsymbol{0} \text{ on } \Gamma_{ext,D} \right\},$$

where

$$a\left(\boldsymbol{u}, \delta\boldsymbol{u}\right) \overset{\text{def}}{=} \int_{\Omega} \boldsymbol{\sigma} \; : [\delta\boldsymbol{u} \otimes \boldsymbol{\nabla}] \, \mathrm{d}\,\Omega, \tag{3}$$

$$b\left(\boldsymbol{t}\left([\![\boldsymbol{u}]\!]\right), \delta\boldsymbol{u}\right) \overset{\text{def}}{=} \int_{\Gamma^{+}_{int}} \boldsymbol{t}\left([\![\boldsymbol{u}]\!]\right) \cdot [\![\delta\boldsymbol{u}]\!] \, \mathrm{d}\,\Gamma, \tag{4}$$

$$l\left(\delta\boldsymbol{u}\right) \overset{\text{def}}{=} \int_{\Gamma_{ext,N}} \hat{\boldsymbol{t}} \cdot \delta\boldsymbol{u} \, \mathrm{d}\,\Gamma, \tag{5}$$

and $\boldsymbol{t}\left([\![\boldsymbol{u}]\!]\right)$ denotes the cohesive zone response. We note that the cohesive zone law $\boldsymbol{t}([\![\boldsymbol{u}]\!])$ is given on stiffness format, thereby allowing softening to be included in the cohesive zone law. For the representation of Γ_{int}, intrinsic interface elements will be used in the present work. The bulk material will be discretized using 3-node and 6-node triangles. The discrete version of Eq. (2) is then obtained by finding $\boldsymbol{u}_h \in \mathbb{U}_h$ such that

$$a\left(\boldsymbol{u}_h, \delta\boldsymbol{u}_h\right) - b\left(\boldsymbol{t}\left([\![\boldsymbol{u}_h]\!]\right), \delta\boldsymbol{u}_h\right) = l\left(\delta\boldsymbol{u}_h\right) \;\; \forall \delta\boldsymbol{u}_h \in \mathbb{U}^{0}_{h}. \tag{6}$$

Eq. (6) represents the conventional displacement based format, where $\boldsymbol{t}$ is given directly in terms of $[\![\boldsymbol{u}]\!]$ by the cohesive zone law. In the following, alternative ways to treat $\boldsymbol{t}$ will be considered.

2.2. *Nonconventional and conventional mixed formats*

As a basis for the weak penalty formulation that will be derived later, we will here develop two alternatives to Eq. (6). To this end, consider first a (nonconventional) mixed format with the displacement jump $\boldsymbol{d}_{\lambda}$ over the crack as an additional unknown field. To establish such a mixed formulation, introduce the forms

$$c\left(\boldsymbol{u}, \delta\boldsymbol{d}_\lambda\right) \stackrel{\text{def}}{=} \int_{\Gamma^+} [\![\boldsymbol{u}]\!] \cdot \delta\boldsymbol{d}_\lambda \, \mathrm{d}\,\Gamma, \tag{7}$$

$$d\left(\boldsymbol{d}_\lambda, \delta\boldsymbol{d}_\lambda\right) \stackrel{\text{def}}{=} \int_{\Gamma^+} \boldsymbol{d}_\lambda \cdot \delta\boldsymbol{d}_\lambda \, \mathrm{d}\,\Gamma. \tag{8}$$

A mixed formulation (on discrete form) with displacements $\boldsymbol{u}_h$ and interface jumps $\boldsymbol{d}_{\lambda,h}$ as unknown fields then reads: Find $\boldsymbol{u}_h \in \mathbb{U}_h$ and $\boldsymbol{d}_{\lambda,h} \in \mathbb{D}_h$ such that

$$a\left(\boldsymbol{u}_h, \delta\boldsymbol{u}_h\right) - b\left(\boldsymbol{t}(\boldsymbol{d}_{\lambda,h}), \delta\boldsymbol{u}_h\right) = l\left(\delta\boldsymbol{u}_h\right) \;\; \forall \delta\boldsymbol{u}_h \in \mathbb{U}_h^0, \tag{9}$$

$$-c\left(\boldsymbol{u}_h, \delta\boldsymbol{d}_{\lambda,h}\right) + d\left(\boldsymbol{d}_{\lambda,h}, \delta\boldsymbol{d}_{\lambda,h}\right) = 0 \qquad \forall \delta\boldsymbol{d}_{\lambda,h} \in \mathbb{D}_h, \tag{10}$$

where we note that no modifications to the cohesive zone model are needed: it is still given on stiffness format by computing $\boldsymbol{t}(\boldsymbol{d}_{\lambda,h})$.

As a second alternative, a conventional mixed formulation can be established by instead introducing the traction $\boldsymbol{t}_\lambda$ as an additional unknown field, see e.g. [8]. The task is then to find $\boldsymbol{u}_h \in \mathbb{U}_h$ and $\boldsymbol{t}_{\lambda,h} \in \mathbb{D}_h$ such that

$$a\left(\boldsymbol{u}_h, \delta\boldsymbol{u}_h\right) - b\left(\boldsymbol{t}_{\lambda,h}, \delta\boldsymbol{u}_h\right) = l\left(\delta\boldsymbol{u}_h\right) \;\; \forall \delta\boldsymbol{u}_h \in \mathbb{U}_h^0, \tag{11}$$

$$-b\left(\delta\boldsymbol{t}_{\lambda,h}, \boldsymbol{u}_h\right) + c\left(\boldsymbol{d}(\boldsymbol{t}_{\lambda,h}), \delta\boldsymbol{t}_{\lambda,h}\right) = 0 \; \forall \delta\boldsymbol{t}_{\lambda,h} \in \mathbb{D}_h, \tag{12}$$

where $\boldsymbol{d}(\boldsymbol{t}_{\lambda,h})$ denotes the cohesive zone response on compliance format. It is noted that the mixed form given by Eqs. (11) and (12) has the advantage of being symmetric, but it has the disadvantage that the cohesive zone response must be expressed on compliance format, leading to additional difficulties for cohesive zone models with softening.

2.3. Weak penalty format

2.3.1. Preliminaries

Here, we will derive a weak penalty formulation from the (nonstandard) mixed format given by Eqs. (9) and (10). It will also be shown that the conventional mixed format given by Eqs. (11) and (12) leads to an identical weak penalty formulation, however under more restrictive assumptions on the cohesive zone constitutive model.

To establish a weak penalty formulation, we follow along the lines of [12] and introduce a projection operator π_D denoting the orthogonal projection onto the space $\mathbb{D}_h$. More precisely, π_D has the property that for any $\boldsymbol{v} \in [\mathbb{L}_2\left(\Omega\right)]^d$,

$$\int_{\Gamma^+} \left[\boldsymbol{v} - \pi_D\left(\boldsymbol{v}\right)\right] \cdot \delta\boldsymbol{d} \, \mathrm{d}\,\Gamma = 0 \; \forall \delta\boldsymbol{d} \in \mathbb{D}_h. \tag{13}$$

π_D can be interpreted as a coarsening operator, since it projects $\boldsymbol{v}$ onto $\mathbb{D}_h$. The interpretation of π_D as a coarsening operator is important, because the inf–sup condition can be fulfilled by choosing $\mathbb{D}_h$ coarse enough. See p. 216 in [12] for further details and [13] for a more general discussion.

As will be seen below, the projection operator π_D can be used to eliminate the second equation in the mixed formulation, leading to a weak penalty formulation with $\boldsymbol{u}_h$ as single unknown field.

2.3.2. Derivation from nonstandard format

To derive a weak penalty formulation from the nonstandard mixed format given by Eqs. (9) and (10), we first note that Eq. (10) holds if $\boldsymbol{d}_{\lambda,h} = \pi_D\left([\![\boldsymbol{u}_h]\!]\right)$, where π_D is the projection operator introduced above. Hence, a weak penalty formulation can be obtained by inserting $\boldsymbol{d}_{\lambda,h} = \pi_D\left([\![\boldsymbol{u}_h]\!]\right)$ in Eq. (9) to obtain

$$a\left(\boldsymbol{u}_h, \delta\boldsymbol{u}_h\right) - b\left(\boldsymbol{t}(\pi_D\left([\![\boldsymbol{u}_h]\!]\right)), \delta\boldsymbol{u}_h\right) = l\left(\delta\boldsymbol{u}_h\right) \;\; \forall \delta\boldsymbol{u}_h \in \mathbb{U}_h^0, \tag{14}$$

which can be solved for the single unknown field $\boldsymbol{u}_h$. If no coarsening is performed by π_D, we have $\pi_D\left([\![\boldsymbol{u}_h]\!]\right) = [\![\boldsymbol{u}_h]\!]$ and the conventional displacement based format given by Eq. (6) is retrieved. However, choosing a reduced space $\mathbb{D}_h$ allows coarsening of the approximation space for the cohesive zone contribution in order to obtain a stable formulation. The weakly penalized formulation given by Eq. (14) is computationally attractive for several reasons:

1. The equation can be solved for the single unknown field $\boldsymbol{u}_h$: no additional unknowns need to be introduced. This reduces the computational cost compared to a mixed formulation.

2. Since the weakly penalized formulation given by Eq. (14) is equivalent to the mixed formulation given by Eqs. (9) and (10), we may choose a stable space $\mathbb{D}_h$ to obtain results free from spurious traction oscillations as discussed further below.
3. No modifications to the cohesive zone model are needed, since it appears on stiffness format in Eq. (14). In particular, softening in the cohesive zone can be handled using this formulation.

2.3.3. Derivation from conventional format

To see that a weak penalty formulation identical to Eq. (14) can be derived from the conventional format given by Eqs. (11) and (12), first recall that Eq. (12) reads

$$\int_{\Gamma^+} \delta \boldsymbol{t}_{\lambda,h} \cdot \left([\![\boldsymbol{u}_h]\!] - \boldsymbol{d}(\boldsymbol{t}_{\lambda,h}) \right) \mathrm{d}\,\Gamma = 0 \; \forall \delta \boldsymbol{t}_{\lambda,h} \in \mathbb{D}_h, \tag{15}$$

which holds if

$$\boldsymbol{d}(\boldsymbol{t}_{\lambda,h}) = \pi_D [\![\boldsymbol{u}_h]\!]. \tag{16}$$

Applying the cohesive zone constitutive law to Eq. (16) gives

$$\boldsymbol{t}(\boldsymbol{d}(\boldsymbol{t}_{\lambda,h})) = \boldsymbol{t}(\pi_D [\![\boldsymbol{u}_h]\!]). \tag{17}$$

If $\boldsymbol{d}(\boldsymbol{t}_{\lambda,h})$ is uniquely determined,[1] then $\boldsymbol{t}(\boldsymbol{d}(\boldsymbol{t}_{\lambda,h})) = \boldsymbol{t}_{\lambda,h}$, so that $\boldsymbol{t}_{\lambda,h} = \boldsymbol{t}(\pi_D [\![\boldsymbol{u}_h]\!])$. Inserting in Eq. (11) gives

$$a\,(\boldsymbol{u}_h, \delta \boldsymbol{u}_h) - b\,(\boldsymbol{t}(\pi_D [\![\boldsymbol{u}_h]\!]), \delta \boldsymbol{u}_h) = l\,(\delta \boldsymbol{u}_h) \;\; \forall \delta \boldsymbol{u}_h \in \mathbb{U}_h^0, \tag{18}$$

which can be solved for the single unknown field $\boldsymbol{u}_h$.

2.3.4. Discussion

As can be seen, the weak penalty formulation given by Eq. (18) is identical to the formulation given by Eq. (14). It is emphasized that the derivation leading to Eq. (14) is more general, since the nonstandard mixed format given by Eqs. (9) and (10) is valid for all cohesive zone constitutive models that can be expressed on stiffness format, whereas the conventional mixed format given by Eqs. (11) and (12) only can be used with cohesive zone constitutive models that can be expressed on compliance format.

2.4. The inf–sup condition and traction oscillations

2.4.1. Preliminaries

When solving a mixed problem such as the nonconventional mixed format given by Eqs. (9) and (10), or the conventional mixed format given by Eqs. (11) and (12), a stable, oscillation-free solution is obtained by ensuring fulfillment of the inf–sup (LBB) condition. This stability requirement applies also to the weak penalty formulation: a pair of spaces $\mathbb{U}_h^0$ and $\mathbb{D}_h$ that give a stable solution for the mixed problem, will give a stable solution also for the corresponding weak penalty formulation, see [12] for further discussion. Since Eqs. (14) and (18) are identical, we may evaluate the stability of the weak penalty formulation by studying the inf–sup condition either for the nonconventional mixed form given by Eqs. (9) and (10) or the conventional mixed form given by Eqs. (11) and (12). Due to the wealth of results available in the literature, we prefer to study the inf–sup condition for the conventional mixed form.[2]

As a basis for the following discussion, we recall that $b\,(\cdot, \cdot)$ is given by

$$b\left(\boldsymbol{t}_{\lambda,h}, \boldsymbol{u}_h\right) = \int_{\Gamma_{int}^+} \boldsymbol{t}_{\lambda,h} \cdot [\![\boldsymbol{u}_h]\!] \,\mathrm{d}\,\Gamma, \tag{19}$$

[1] This is not the case for constitutive models accounting for softening.

[2] Evaluation of the inf–sup condition for unsymmetric mixed forms like the nonstandard mixed form proposed here is also possible, see e.g. [14]. However, the inf–sup condition for unsymmetric problems is only seldom discussed in the literature.

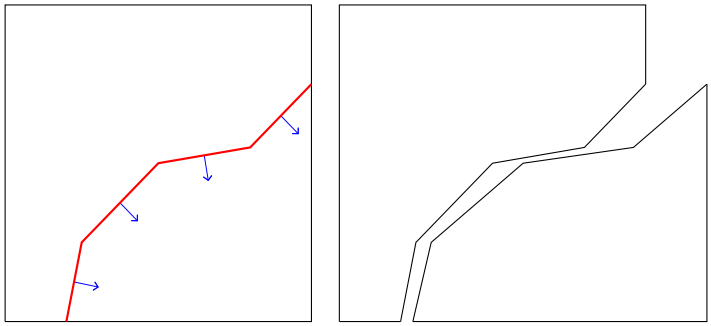

(a) Undeformed geometry. (b) Deformed geometry.

Fig. 2. Example geometry for illustration of stability problems.

and we note the analogy with contact problems [15] as well as with weakly periodic boundary conditions [16,17]. The inf–sup condition is fulfilled if $\exists \beta > 0$ such that

$$\inf_{\mathbf{0}\neq \boldsymbol{t}_{\lambda,h}\in\mathbb{D}_h} \sup_{\mathbf{0}\neq \boldsymbol{u}_h\in\mathbb{U}_h^0} \frac{b\left(\boldsymbol{t}_{\lambda,h}, \boldsymbol{u}_h\right)}{\|\boldsymbol{t}_{\lambda,h}\|_{\mathbb{D}_h}\|\boldsymbol{u}_h\|_{\mathbb{U}_h^0}} \geq \beta, \tag{20}$$

where the positive constant β is independent of the mesh size. Furthermore, $\|\cdot\|_{\mathbb{D}_h}$ and $\|\cdot\|_{\mathbb{U}_h^0}$ are the norms pertinent to $\mathbb{D}_h$ and $\mathbb{U}_h^0$, respectively. We note, again, that $b(\cdot,\cdot)$ as given by Eq. (19) takes exactly the same form as for contact problems [15] and weakly periodic boundary conditions [16,17]. Hence, when identifying stable choices for $\mathbb{U}_h^0$ and $\mathbb{D}_h$, stability results from the literature can be exploited as discussed further below.

Turning our attention to the evaluation of $\boldsymbol{t}$ along Γ_{int}^+, we note that an anisotropic cohesive zone law will introduce traction discontinuities where the interface normal is discontinuous (that is, between interface elements). Hence, $\boldsymbol{t}(\pi_D[\![\boldsymbol{u}_h]\!])$ may be discontinuous along Γ_{int}^+ even if $\pi_D[\![\boldsymbol{u}_h]\!]$ is continuous over element edges. Furthermore, $\boldsymbol{t}(\pi_D[\![\boldsymbol{u}_h]\!])$ may be discontinuous if material properties in the cohesive zone (e.g. stiffness or damage) vary along the interface.

In the following, we consider the common case of a piecewise linear continuous displacement approximation and investigate why full Gauss integration, two-point Lobatto integration and one-point Gauss integration sometimes fail.

2.4.2. *Traction oscillations in standard interface elements*

To discuss the traction oscillations sometimes seen in interface elements in light of the inf–sup condition, first consider a standard displacement based penalty formulation implying that no restriction is done by the projection π_D in Eq. (18), i.e. $\boldsymbol{u}_h$ is solved from

$$a(\boldsymbol{u}_h, \delta\boldsymbol{u}_h) - b(\boldsymbol{t}([\![\boldsymbol{u}_h]\!]), \delta\boldsymbol{u}_h) = l(\delta\boldsymbol{u}_h) \;\; \forall \delta\boldsymbol{u}_h \in \mathbb{U}_h^0. \tag{21}$$

For this case, the (implicitly chosen) approximation space for $\boldsymbol{t}$ is completely dictated by $\mathbb{U}_h$. As an example,[3] consider a specimen with a discretized crack as shown in Fig. 2(a), where the normal direction is discontinuous between interface elements. Assume that the left piece of the specimen is fixed, and that the right piece is deformed according to $u_x = 0.2x$ as shown in Fig. 2(b). For simplicity, assume that the cohesive zone material is elastic with normal stiffness $k_n = 1$. With this simple example in mind, we now consider different alternatives for the integration of the cohesive zone response.

Full Gauss integration. Using full integration and a piecewise linear displacement approximation, the interface jump expressed in global coordinates will be piecewise linear and continuous between interface elements. However, the *normal component* of the interface jump will be discontinuous between interface elements as shown in Fig. 3(a) for the example discussed above. Hence, the normal component of the traction will also be discontinuous between interface elements. Therefore, we have a piecewise linear continuous approximation for $\boldsymbol{u}$ and a piecewise linear

[3] The analysis does not rely on this example, it is shown only to give an explicit illustration of the idea.

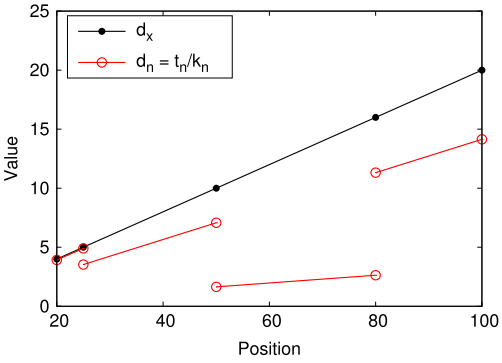

(a) Full (Gauss) integration. Note that the normal jump d_n and the normal traction t_n have discontinuities at points where the global components of the displacement jump (e.g. d_x) are continuous.

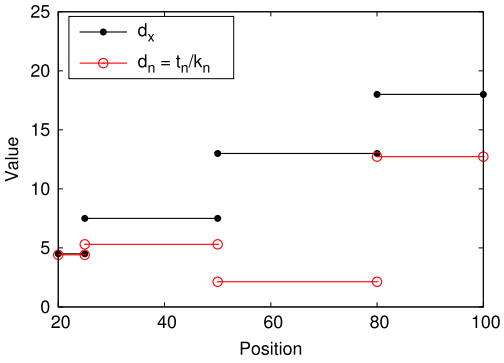

(b) One point integration.

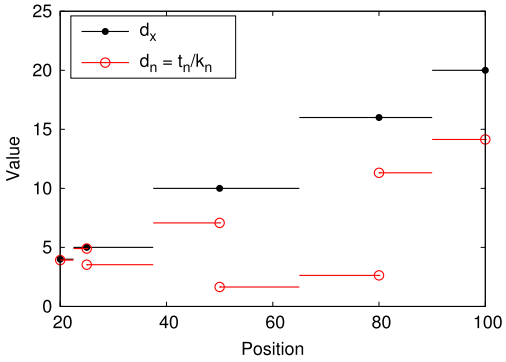

(c) Lobatto integration. Note that the normal jump d_n and the normal traction t_n have discontinuities at points where the global components of the displacement jump (e.g. d_x) are continuous.

Fig. 3. Interface jump and traction using different integration schemes for the illustration example involving a curved crack considered in Section 2.4.2. In the figures, $d_x = u_x^+ - u_x^-$, $d_n = \left[\boldsymbol{u}^+ - \boldsymbol{u}^-\right] \cdot \boldsymbol{n}$, and the circles represent node locations.

discontinuous approximation for $\boldsymbol{t}$. This combination violates the inf–sup condition and is therefore unstable: to have stable response with discontinuous traction, the traction approximation needs to be two orders lower than the displacement approximation (see p. 181 in [18] and exploit the analogy with the contact problem) or, as an alternative, the traction elements can be made coarser than the displacement elements in a suitable way (see e.g. [13,17]).

Note however, that for an *isotropic* elastic cohesive zone, the traction is independent of the normal direction and therefore continuous between interface elements. Hence, for the special case of an *isotropic* cohesive zone, the approximations for $\boldsymbol{u}_h$ and $\boldsymbol{t}_{\lambda,h}$ span exactly the same space and we expect stable response [18].

One-point Gauss integration. One-point integration corresponds to piecewise constant interface jump and traction on each interface element as illustrated in Fig. 3(b). A piecewise constant traction on each linear displacement element is known to violate the inf–sup condition [18]. Hence, one-point integration is expected to give stability problems for both isotropic and anisotropic cohesive zone laws.

Two-point Lobatto integration. Two-point Lobatto integration gives the same result as a piecewise constant traction approximation with traction discontinuities at element centers. (See Appendix A for a proof of this claim.) For a straight crack with an isotropic cohesive zone, where experience has shown that two-point Lobatto integration works well [1], the traction will be continuous over nodes and only have discontinuities at element centers. However, for a curved crack in combination with an anisotropic cohesive zone, the traction will have discontinuities also at nodes where the normal changes discontinuously as shown in Fig. 3(c) for the illustration example. Hence, Lobatto integration is expected to be unstable for curved cracks with anisotropic cohesive zones.

2.4.3. Stable choices for $\mathbb{D}_h$ and construction of π_D

To alleviate spurious traction oscillations by using a weak penalty formulation and choosing a stable approximation space $\mathbb{D}_h$, we first recall that $\boldsymbol{t}_{\lambda,h}$ may contain discontinuities as discussed above. Hence, we wish to identify choices for $\mathbb{D}_h$ that allow discontinuities.

As a first alternative, note that for a quadratic displacement approximation, a stable choice is to let $\mathbb{D}_h$ contain functions that are piecewise constant on each element [14,18,7]. This choice allows the projection π_D to be constructed locally on each element.[4] From Eq. (13), we require

$$\int_{\Gamma^+} \pi_D(\boldsymbol{v}) \cdot \delta\boldsymbol{d} \,\mathrm{d}\,\Gamma = \int_{\Gamma^+} \boldsymbol{v} \cdot \delta\boldsymbol{d} \,\mathrm{d}\,\Gamma \;\forall \delta\boldsymbol{d} \in \mathbb{D}_h. \tag{22}$$

For an arbitrary interface element, we may set the components of $\delta\boldsymbol{d}$ to one on the element under consideration and zero on all other elements. Letting Γ_e denote the interface element under consideration, we then have

$$\int_{\Gamma_e^+} \pi_D(\boldsymbol{v}) \,\mathrm{d}\,\Gamma = \int_{\Gamma_e^+} \boldsymbol{v} \,\mathrm{d}\,\Gamma. \tag{23}$$

Since $\pi_D(\boldsymbol{v})$ is a constant vector on Γ_e^+, we obtain

$$\pi_D(\boldsymbol{v}) = \frac{1}{|\Gamma_e^+|} \int_{\Gamma_e^+} \boldsymbol{v} \,\mathrm{d}\,\Gamma, \tag{24}$$

where $|\Gamma_e^+| \overset{\text{def}}{=} \int_{\Gamma_e^+} \mathrm{d}\,\Gamma$.

As a second alternative, we can use a linear displacement approximation and let $\mathbb{D}_h$ consist of functions that are piecewise constant over two (displacement) elements. This choice was analyzed for weakly periodic boundary conditions in [17] and a similar approach in the context of XFEM, but for linear functions, can be found in [9]. For this case, the projection is computed from Eq. (24) with the difference that the interface element Γ_e now spans over two displacement elements.

These two alternatives lead to stable results for cases where standard interface elements suffer from spurious traction oscillations, as demonstrated by the numerical examples presented below.

3. Numerical examples

3.1. Preliminaries

This section gives three numerical examples to illustrate the spurious traction oscillations occurring when applying both full integration, Lobatto integration and one-point integration to standard interface elements. It is also shown that the weak penalty formulation proposed in the present work, i.e. Eq. (14) with π_D given by Eq. (24), leads to stable results in these cases.

A linear elastic bulk material will be used in all examples, whereas two different cohesive zone models will be considered. The first cohesive zone model under consideration is a linear elastic isotropic model giving the traction as $\boldsymbol{t} = k\boldsymbol{d}$, where k is the isotropic stiffness of the cohesive zone. The second model considered is an anisotropic linear elastic model, where the traction expressed in the local coordinate system of the element is given by $\boldsymbol{t}_{loc} = \mathbf{K} \cdot \boldsymbol{d}_{loc}$ and

$$\mathbf{K} \overset{\text{def}}{=} \begin{bmatrix} k_s & 0 & 0 \\ 0 & k_s & 0 \\ 0 & 0 & k_n \end{bmatrix}, \tag{25}$$

where k_s is the shear stiffness and k_n is the normal stiffness.

The model proposed in the present work has been implemented in the open source software package OOFEM [19,20].

[4] Note, however, that π_D will have global character in the general case.

3.2. Circular crack

The analysis in Section 2.4.2 indicates that both full Gauss integration and two-point Lobatto integration should give smooth traction profiles for a curved crack with an isotropic cohesive zone (and constant material parameters), whereas oscillations may appear for a curved crack with an anisotropic cohesive zone. To show that these schemes indeed produce oscillatory results, and that the weak penalty formulation is stable, we consider a square specimen with a half circle shaped cohesive surface as shown in Fig. 4(a). The side length of the specimen is $L = 100$ mm and the diameter of the half circle is $d = 60$ mm. The left edge is clamped in both vertical and horizontal directions, whereas the right edge is clamped in vertical direction and a uniform displacement of $u_0 = -1$ mm is prescribed in horizontal direction (i.e. the specimen is compressed). Plane stress is assumed and the bulk material is linear elastic with $E = 20 \times 10^3$ MPa and $\nu = 0.2$. For the cohesive zone, two different material models are studied: an isotropic linear elastic model with stiffness $k = 1 \times 10^{11}$ N mm^{-3} and an anisotropic linear elastic model with normal stiffness $k_n = 1 \times 10^{11}$ N mm^{-3} and shear stiffness $k_s = 1 \times 10^9$ N mm^{-3}. The bulk material is discretized using 3-node triangles, and we consider a coarse mesh consisting of 202 elements as shown in Fig. 4(b), as well as a fine mesh consisting of 36 652 elements (not shown). The results shown below are for the coarse mesh, unless stated otherwise. Using this case setup, the problem is first solved using standard interface elements with full integration, Lobatto integration and one-point integration. Then, the problem is solved using the linear and the quadratic version of the weak penalty formulation proposed in the present work. These models are compared by monitoring the interface traction in normal direction along the cohesive surface (Fig. 5).

Fig. 5(a) shows the normal traction along the circle computed with the isotropic model using standard interface elements, with full integration, one-point integration and two-point Lobatto integration, respectively. As can be seen, both full Gauss integration and two-point Lobatto integration give non-oscillating traction profiles for this case. The non-oscillating response is expected from the theoretical analysis, whereas the step-like appearance of the curves is due to the relatively coarse mesh in combination with the discontinuous surface normal. Furthermore, we note that one-point Gauss quadrature also gives a non-oscillating traction profile, even though this cannot be expected in the general case as discussed further below.

Turning our attention to the results obtained with the anisotropic cohesive zone (and the same integration schemes as for the isotropic case), as shown in Fig. 5(b), we first note that a smooth traction profile is predicted using one-point Gauss quadrature; a result which agrees with its proposal as a strategy to reduce traction oscillations in contact problems [21]. However, one-point Gauss quadrature cannot be expected to give stable results in the general case, as shown by the examples below. Regarding fully integrated interface elements, it can be seen that such elements in combination with the anisotropic model lead to severe oscillations: the amplitude of the fluctuation is roughly four times greater than the magnitude of the response obtained with one-point quadrature. These highly problematic oscillations are actually expected, since fully integrated elements do not fulfill the inf–sup condition for this case, and since stability problems have been reported previously for such elements [1]. More interestingly, Fig. 5(b) shows that Lobatto integration also leads to severe oscillations when anisotropic cohesive zone models are used. Despite the fact that Lobatto integration has previously been proposed as a remedy for traction oscillations, the unstable response of this scheme is expected in light of the discussion in Section 2.4.2.

Fig. 5(c) shows the response obtained using the weak penalty formulation. As can be seen, stable traction profiles are obtained with both the linear and the quadratic version of the formulation. Furthermore, this observation holds for both coarse and fine meshes. Hence, we conclude that even though both Lobatto integration and full integration on standard elements lead to severe spurious oscillations for this case, the weak penalty formulation is stable.

3.3. Grain structure prototype

Interface elements can be used to model intergranular fracture in metal microstructures by inserting such elements at the grain boundaries. To investigate the occurrence of traction oscillations in this type of application, we consider the simple grain structure in Fig. 6(a), consisting of four grains with cohesive zones between the grains. The bulk material is discretized using 942 triangles as shown in Fig. 6(b). The side length of the square specimen is $L = 100$ mm and the grain boundaries are defined by the points $\boldsymbol{p}_1 - \boldsymbol{p}_5$ given in Table 1. The left edge is clamped, whereas a nonuniform

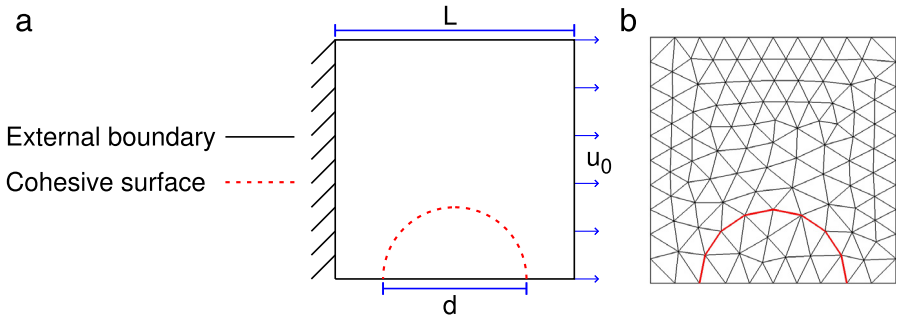

Fig. 4. Geometry and mesh for Example 3.2.

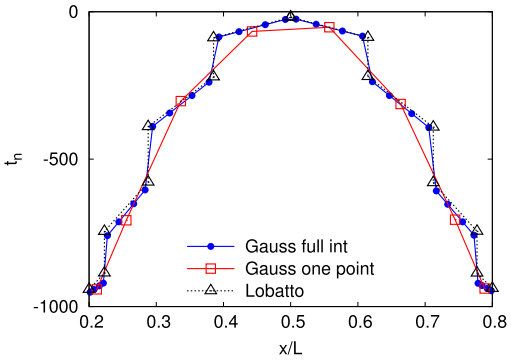

(a) Standard format with isotropic cohesive zone.

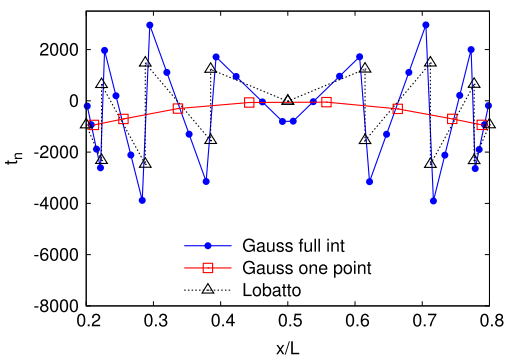

(b) Standard format with anisotropic cohesive zone.

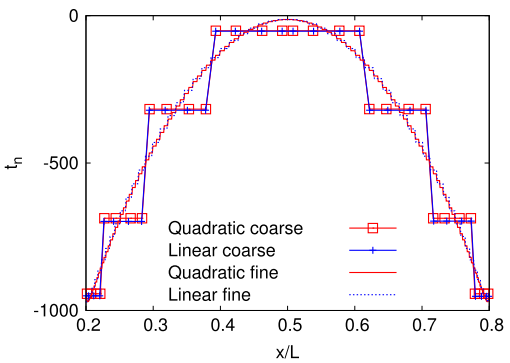

(c) Weak penalty format with anisotropic cohesive zone.

Fig. 5. Interface normal traction along a half circle shaped cohesive interface studied in Example 3.2.

displacement is prescribed on the right edge according to

$$u_x = 0.5 - 2y/L, \tag{26}$$

$$u_y = -2y/L. \tag{27}$$

Plane stress is assumed and the bulk material is linear elastic with $E = 20 \times 10^3$ MPa and $\nu = 0.2$. For the cohesive zone, we consider the anisotropic elastic model described previously with normal stiffness $k_n = 1 \times 10^{11}$ N mm^{-3} and shear stiffness $k_s = 1 \times 10^5$ N mm^{-3}. As in the previous example, the problem is first solved using standard interface elements, with full integration, one-point integration and two-point Lobatto integration, respectively. Then, the problem is solved using the linear and the quadratic version of the weak penalty formulation. These models are again compared by monitoring the normal component of the interface traction (Fig. 7).

Table 1
Points defining the grain boundaries in Example 3.3.

Point	x/L	y/L
$\boldsymbol{p}_1$	0.55	0.6
$\boldsymbol{p}_2$	0.35	0
$\boldsymbol{p}_3$	1	0.65
$\boldsymbol{p}_4$	0.4	1
$\boldsymbol{p}_5$	0	0.5

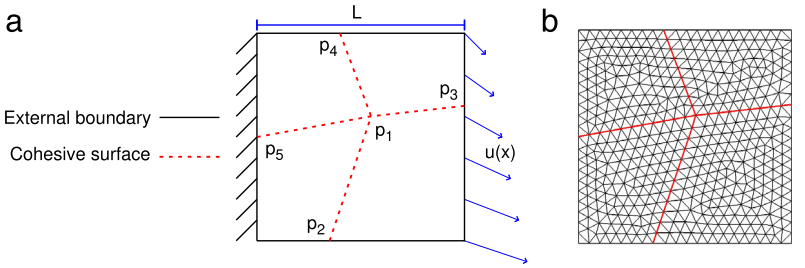

Fig. 6. Geometry and mesh for Example 3.3.

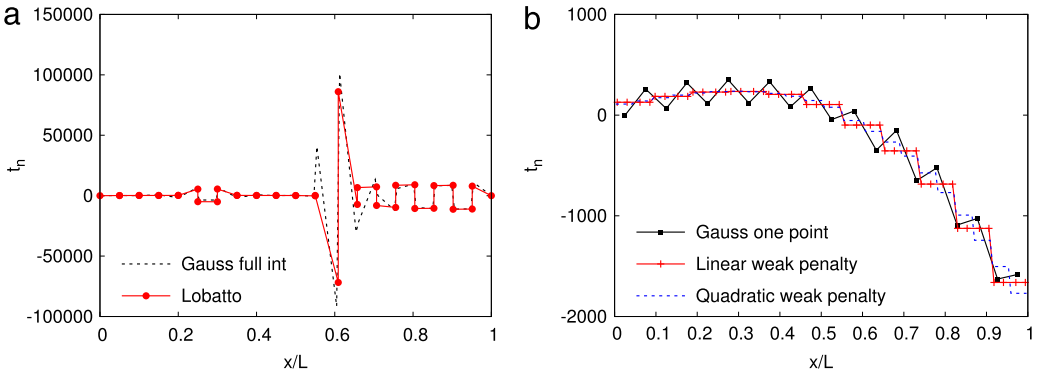

Fig. 7. Interface normal traction along grain boundaries in Example 3.3.

Fig. 7(a) shows the normal traction along the grain boundaries $\boldsymbol{p}_5 - \boldsymbol{p}_1 - \boldsymbol{p}_3$, computed with Lobatto integration and full integration. As can be seen, these schemes both give rise to severe traction oscillations. In particular, a catastrophic overshoot can be seen where the four grains meet in the point $\boldsymbol{p}_1$. This problem at the grain boundary intersection is expected in light of the discussion in Section 2.4.2, since the normal direction of the cohesive surface changes discontinuously here. (In fact, the normal direction is not even well defined in points like $\boldsymbol{p}_1$.) Turning our attention to the response computed with the remaining schemes as shown in Fig. 7(b) (and noting the large difference in scale on the y-axis between Fig. 7(a) and b), we see that one-point quadrature gives rise to light traction oscillations for this case. On the other hand, the weak penalty formulations both give non-oscillating response. For this application, we therefore conclude that both full integration, two-point Lobatto integration and one-point integration give rise to traction oscillations, whereas the weak penalty formulations are stable.

3.4. Bending of notched beam

As a final example, we consider a 2D version of the notched beam studied in [1]. The beam, which is shown in Fig. 8, has total length $L = 450$ mm, height $H = 100$ mm, out of plane thickness 100 mm and notch length $a = 20$ mm. The notch can be seen as the limiting case of a discontinuously changing cohesive zone stiffness, where this stiffness instantly drops to zero at the notch. Hence, this case represents the case of a discontinuous traction induced by discontinuously changing material parameters. The bulk material is linear elastic with Young's modulus $E = 20 \times$

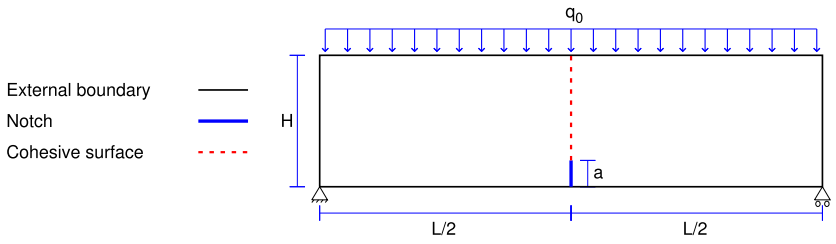

Fig. 8. Notched beam considered in Example 3.4.

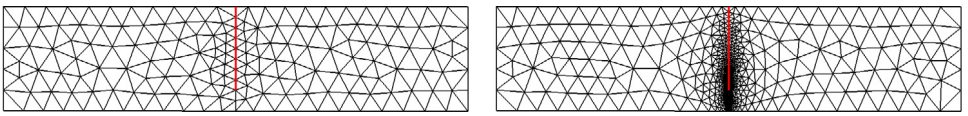

(a) Coarse mesh (297 bulk elements). (b) Fine mesh (2458 bulk elements).

Fig. 9. Meshes used in Example 3.4.

10^3 MPa and Poisson's ratio $\nu = 0.2$. The cohesive zone material is linear elastic with stiffness $k = 1 \times 10^7$ N mm^{-3}. A distributed load is applied on the top edge such that the total force applied is 1 kN. A coarse mesh (297 elements) and a fine mesh (2458 elements) are considered as shown in Fig. 9. As in the previous examples, the problem is first solved using standard interface elements, with full integration, one-point integration and two-point Lobatto integration, respectively. Then, the problem is solved using the linear and the quadratic version of the weak penalty formulation. Again, these approaches are compared by studying the normal component of the interface traction (Fig. 10).

Fig. 10(a) shows the normal traction along the interface computed with full Gauss integration. The response obtained with the coarse mesh shows a spike close to the crack tip as also observed in [1]. Interestingly, this spike does not reduce under mesh refinement: for the finer mesh, the strength of the oscillation is so large that the normal traction takes negative values close to the crack tip. Comparing this spike to the results computed with one-point Gauss integration as shown in Fig. 10(b), it can be seen that the one-point integration leads to very strong oscillations for this case. As for the full integration, the oscillations are more severe for the finer mesh. Hence, these oscillations cannot be reduced by refining the mesh, neither for full integration nor for one-point integration. In contrast, we note that two-point Lobatto integration performs very well for this case as shown in Fig. 10(c): a result which is in agreement with [1]. However, this good performance cannot be expected in the general case as demonstrated by the previous examples. Turning our attention to the results obtained with the weak penalty formulation as shown in Fig. 10(d), we note that the results are good also for this case, even though a small kink can be seen at $y = 20$ for the fine mesh. This kink, which is much smaller than the kink seen in Fig. 10(a), is probably a result of the singularity in the stress field at $y = 20$. Nevertheless, the weak penalty formulation performs very well compared to full integration and one-point integration. It can therefore be concluded that full integration and one-point integration lead to catastrophic oscillations for this case, whereas Lobatto integration and the weak penalty formulation lead to acceptable results.

4. Conclusions

In this paper, spurious traction oscillations in intrinsic interface elements are discussed. It is shown that these oscillations are related to violation of the inf–sup (LBB) condition and a remedy using a weak penalty formulation is proposed.

Based on the analysis of the inf–sup condition, the occurrence of traction oscillations for the standard displacement based formulation is discussed: in addition to the oscillations reported in previous research when applying full Gauss integration [1], it is shown that oscillations may also appear when using two-point Lobatto integration and one-point integration. This is an important observation, because these two methods have been previously proposed as remedies for traction oscillations [1,21]. While the results confirm the non-oscillating behavior of Lobatto integration for the straight crack studied in [1], it is shown that both this integration scheme and full Gauss integration may lead to severe oscillations for curved or intersecting cracks with anisotropic cohesive zone models. Furthermore, the results indicate that one-point integration may work well for some cases involving curved cracks, whereas severe oscillations

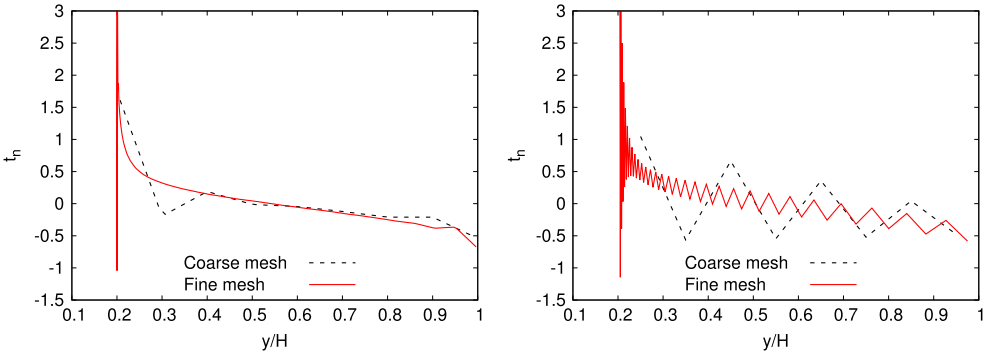

(a) Full Gauss integration.

(b) One point Gauss integration.

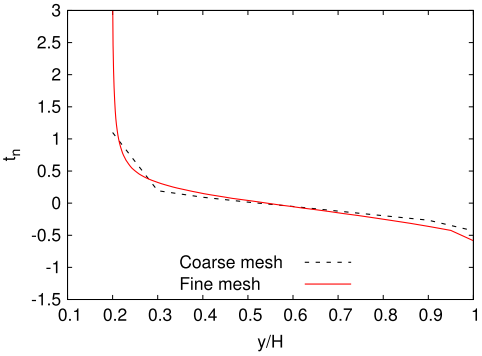

(c) Lobatto.

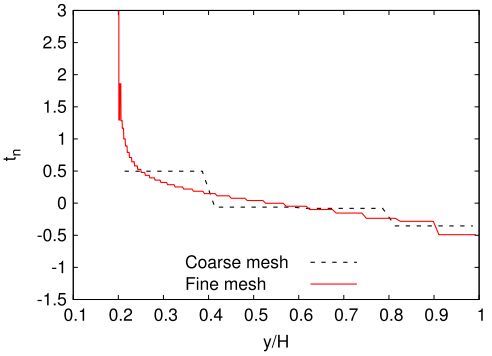

(d) Linear weak penalty.

Fig. 10. Interface normal traction for Example 3.4.

can occur for straight or intersecting cracks. Thus, attempting to alleviate traction oscillations using the standard displacement based formulation with reduced integration is in general highly problematic.

As a remedy for this, a weak penalty formulation is proposed, that allows the approximation space for the cohesive zone contribution to be chosen such that the inf–sup condition is fulfilled. To be specific, departing from the proposed nonstandard mixed formulation leads to a weak penalty formulation that does not require any modifications to the cohesive zone model. Interestingly, it turns out that an identical weak penalty formulation can be obtained from the standard mixed formulation, however under more restrictive assumptions on the cohesive zone model. Within the setting of the proposed weak penalty formulation, the choice of suitable approximation spaces fulfilling the inf–sup condition is discussed, and two stable piecewise constant approximations are studied: (i) a quadratic displacement approximation in combination with a piecewise constant jump on each displacement element, and (ii) a linear displacement approximation in combination with a piecewise constant jump over two displacement elements. These approximations both give non-oscillating results for straight, curved, and intersecting cracks, as shown by the numerical examples. Despite the restriction to two-dimensional examples in the present work, we note that a piecewise constant jump on each quadratic displacement element can be applied also in 3D. Furthermore, it is emphasized that, apart from the two approximations considered here, other approximations fulfilling the inf–sup condition can also be applied in the proposed framework.

A key observation in the present work is that stability problems may occur for the standard displacement based formulation when the interface traction changes discontinuously between elements. These stability problems have been illustrated by numerical examples where the traction discontinuities are induced by an anisotropic cohesive zone model in combination with a discontinuous interface normal. Apart from a discontinuously changing interface normal, it should be noted that discontinuities may also be induced by spatially varying material parameters or damage evolution in the cohesive zone. Hence, the stability analysis presented here is relevant for a wide range of interface problems, including curved or intersecting cracks, as well as cases involving damage evolution at the interface.

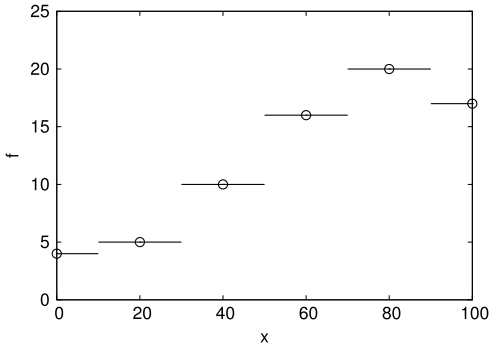

Fig. A.11. Piecewise constant approximation with discontinuities at element centers, which gives the same result as two-point Lobatto integration. The circles denote node locations.

To summarize, the standard displacement based formulation with two-point Lobatto integration seems to work well for straight cracks and isotropic cohesive zones, whereas curved or intersecting cracks require more sophisticated remedies, such as the weak penalty formulation proposed in the present work.

Acknowledgments

The financial support by the Swedish Research Council (www.vr.se), under contract 2012-3006, is gratefully acknowledged. Helpful discussions with Assoc. Prof. Martin Fagerström and Prof. Fredrik Larsson are also greatly appreciated.

Appendix. Lobatto integration interpreted as piecewise constant interpolation

In Section 2.4.2, it was claimed that two-point Lobatto integration gives the same result as a piecewise constant interpolation with discontinuities at element centers. To prove this, consider a function f interpolated by standard linear basis functions N_1 and N_2, related to nodes 1 and 2, respectively. The Finite Element approximation of f reads $f_h = N_1(x)f(x_1) + N_2(x)f(x_2)$. Approximating the integral of f_h over an element using two-point Lobatto integration and noting that $N_1(x_1) = N_2(x_2) = 1$, we have

$$\int_{\Gamma_e} f_h \,\mathrm{d}\,\Gamma \approx wN_1(x_1)f(x_1) + wN_2(x_2)f(x_2) = wf(x_1) + wf(x_2), \tag{A.1}$$

where $w = |\Gamma_e|/2$.

Now, consider instead a piecewise constant approximation for f, with a discontinuity at the element center, given by

$$\begin{aligned} \tilde{f}_h &= \tilde{N}_1(x)f(x_1) + \tilde{N}_2(x)f(x_2), \\ \tilde{N}_1(x) &= 1 - \mathcal{H}(x - x_c), \\ \tilde{N}_2(x) &= \mathcal{H}(x - x_c), \end{aligned} \tag{A.2}$$

where $\mathcal{H}$ denotes the Heaviside function and x_c is the center point of the interface element. (We note that this approximation builds a partition of unity since $\tilde{N}_1(x) + \tilde{N}_2(x) = 1$ and that the Kronecker-δ property is fulfilled since $\tilde{N}_i(x_j) = \delta_{ij}$.) Evaluating the integral of $\tilde{f}_h$ over an element using this interpolation gives

$$\begin{aligned} \int_{\Gamma_e} \tilde{f}_h \,\mathrm{d}\,\Gamma &= \int_{\Gamma_e} \tilde{N}_1(x)f(x_1) + \tilde{N}_2(x)f(x_2) \,\mathrm{d}\,\Gamma \\ &= \int_{x_1}^{x_c} \tilde{N}_1(x)f(x_1) + \tilde{N}_2(x)f(x_2) \,\mathrm{d}\,\Gamma + \int_{x_c}^{x_2} \tilde{N}_1(x)f(x_1) + \tilde{N}_2(x)f(x_2) \,\mathrm{d}\,\Gamma \\ &= \int_{x_1}^{x_c} \tilde{N}_1(x)f(x_1) \,\mathrm{d}\,\Gamma + \int_{x_c}^{x_2} \tilde{N}_2(x)f(x_2) \,\mathrm{d}\,\Gamma \end{aligned}$$

$$= \int_{x_1}^{x_c} f(x_1)\,\mathrm{d}\,\Gamma + \int_{x_c}^{x_2} f(x_2)\,\mathrm{d}\,\Gamma$$
$$= wf(x_1) + wf(x_2), \tag{A.3}$$

where $w = |\Gamma_e|/2$. Since Eqs. (A.1) and (A.3) lead to identical results, we conclude that two-point Lobatto integration can be interpreted as the piecewise constant approximation given by Eq. (A.2). This piecewise constant approximation is shown schematically in Fig. A.11.

References

[1] J.C.J. Schellekens, R. De Borst, On the numerical integrations of interface elements, Internat. J. Numer. Methods Engrg. 36 (1) (1993) 43–66.
[2] V. Kaliakin, J. Li, Insight into deficiencies associated with commonly used zero-thickness interface elements, Comput. Geotech. 17 (2) (1995) 225–252.
[3] A. Simone, Partition of unity-based discontinuous elements for interface phenomena: computational issues, Commun. Numer. Methods. Eng. 20 (6) (2004) 465–478.
[4] F. Hashagen, R. De Borst, An interface element for modelling the onset and growth of mixed-mode cracking in aluminium and fibre metal laminates, Struct. Eng. Mech. 5 (6) (1997) 817–837.
[5] R. de Borst, Numerical aspects of cohesive-zone models, Eng. Fract. Mech. 70 (14) (2003) 1743–1757.
[6] J.T. Oden, N. Kikuchi, Finite element methods for constrained problems in elasticity, Internat. J. Numer. Methods Engrg. 18 (5) (1982) 701–725.
[7] E. Lorentz, A mixed interface finite element for cohesive zone models, Comput. Methods Appl. Mech. Engrg. 198 (2) (2008) 302–317.
[8] F. Cazes, M. Coret, A. Combescure, A two-field modified Lagrangian formulation for robust simulations of extrinsic cohesive zone models, Comput. Mech. 51 (6) (2012) 865–884.
[9] É Béchet, N. Moës, B. Wohlmuth, A stable Lagrange multiplier space for stiff interface conditions within the extended finite element method, Internat. J. Numer. Methods Engrg. 78 (8) (2009) 931–954.
[10] G. Ferté, P. Massin, N. Moës, Interface problems with quadratic X-FEM: design of a stable multiplier space and error analysis, Internat. J. Numer. Methods Engrg. 100 (11) (2014) 834–870.
[11] M. Bercovier, Perturbation of mixed variational problems. Application to mixed finite element methods, RAIRO Anal. Numer. 12 (3) (1978) 211–236.
[12] M. Hadjicharalambous, J. Lee, N.P. Smith, D.A. Nordsletten, A displacement-based finite element formulation for incompressible and nearly-incompressible cardiac mechanics, Comput. Methods Appl. Mech. Engrg. 274 (100) (2014) 213–236.
[13] E. Burman, Projection stabilization of Lagrange multipliers for the imposition of constraints on interfaces and boundaries, Numer. Methods Partial Differential Equations 30 (2) (2014) 567–592.
[14] F. Brezzi, M. Fortin, Mixed and Hybrid Finite Element Methods, Springer, New York, 1991.
[15] N. El-Abbasi, K.-J. Bathe, Stability and patch test performance of contact discretizations and a new solution algorithm, Comput. Struct. 79 (16) (2001) 1473–1486.
[16] F. Larsson, K. Runesson, S. Saroukhani, R. Vafadari, Computational homogenization based on a weak format of micro-periodicity for RVE-problems, Comput. Methods Appl. Mech. Engrg. 200 (1–4) (2011) 11–26.
[17] E. Svenning, M. Fagerström, F. Larsson, Computational homogenization of microfractured continua using weakly periodic boundary conditions, Comput. Methods Appl. Mech. Engrg. 299 (2016) 1–21.
[18] K.J. Bathe, F. Brezzi, Stability of finite element mixed interpolations for contact problems, Rend. Lincei Mat. Appl. 12 (3) (2001) 167–183.
[19] B. Patzák, Z. Bittnar, Design of object oriented finite element code, Adv. Eng. Softw. 32 (10–11) (2001) 759–767.
[20] B. Patzák, OOFEM project home page: www.oofem.org (2000). http://www.oofem.org.
[21] P. Wriggers, Computational Contact Mechanics, Springer, Berlin Heidelberg, 2006, http://www.scopus.com/inward/record.url?eid=2-s2.0-84891471348&partnerID=tZOtx3y1.